

Published in final edited form as:

*J Biomed Mater Res A*. 2012 July ; 100(7): 1792–1802. doi:10.1002/jbm.a.34130.

## Poly(Propylene Fumarate) Reinforced Dicalcium Phosphate Dihydrate Cement Composites for Bone Tissue Engineering

Daniel L. Alge<sup>1</sup>, Jeffrey Bennet<sup>2</sup>, Trevor Treasure<sup>2</sup>, Sherry Voytik-Harbin<sup>1</sup>, W. Scott Goebel<sup>3,4</sup>, and Tien-Min Gabriel Chu<sup>5,\*</sup>

<sup>1</sup>Weldon School of Biomedical Engineering, Purdue University, West Lafayette, IN 47908, USA

<sup>2</sup>Department of Oral Surgery and Hospital Dentistry, Indiana University School of Dentistry, Indianapolis, IN 46202, USA

<sup>3</sup>Herman B Wells Center for Pediatric Research, Indiana University School of Medicine, Indianapolis, IN 46202, USA

<sup>4</sup>Department of Pediatrics, Indiana University School of Medicine, Indianapolis, IN 46202, USA

<sup>5</sup>Department of Restorative Dentistry, Division of Dental Biomaterials, Indiana University School of Dentistry, Indianapolis, IN 46202, USA

### Abstract

Calcium phosphate cements have many desirable properties for bone tissue engineering, including osteoconductivity, resorbability, and amenability to rapid prototyping based methods for scaffold fabrication. In this study, we show that dicalcium phosphate dihydrate (DCPD) cements, which are highly resorbable but also inherently weak and brittle, can be reinforced with poly(propylene fumarate) (PPF) to produce strong composites with mechanical properties suitable for bone tissue engineering. Characterization of DCPD-PPF composites revealed significant improvements in mechanical properties for cements with a 1.0 powder to liquid ratio. Compared to non-reinforced controls, flexural strength improved from  $1.80 \pm 0.19$  MPa to  $16.14 \pm 1.70$  MPa, flexural modulus increased from  $1073.01 \pm 158.40$  MPa to  $1303.91 \pm 110.41$  MPa, maximum displacement during testing increased from  $0.11 \pm 0.04$  mm to  $0.51 \pm 0.09$  mm, and work of fracture improved from  $2.74 \pm 0.78$  J/m<sup>2</sup> to  $249.21 \pm 81.64$  J/m<sup>2</sup>. To demonstrate the utility of our approach for scaffold fabrication, 3D macroporous scaffolds were prepared with rapid prototyping technology. Compressive testing revealed that PPF reinforcement increased scaffold strength from  $0.31 \pm 0.06$  MPa to  $7.48 \pm 0.77$  MPa. Finally, 3D PPF-DCPD scaffolds were implanted into calvarial defects in rabbits for 6 weeks. Although the addition of mesenchymal stem cells to the scaffolds did not significantly improve the extent of regeneration, numerous bone nodules with active osteoblasts were observed within the scaffold pores, especially in the peripheral regions. Overall, the results of this study suggest that PPF-DCPD composites may be promising scaffold materials for bone tissue engineering.

### INTRODUCTION

Bone tissue engineering has produced promising clinical results. It has been shown that bone defects can be repaired using a combination of autologous adult stems cells (i.e. mesenchymal stem cells; MSC) and an osteoconductive scaffold material [1–5]. Nonetheless, the search for better scaffold materials to promote bone regeneration continues. Porous calcium phosphate ceramics (e.g. hydroxyapatite, hydroxyapatite/ $\beta$ -tricalcium

\*Corresponding author Tien-Min Gabriel Chu, D.D.S., Ph.D., Phone: 317-274-5148, Fax: 317-278-7462, tgchu@iupui.edu.

phosphate mixtures) have been used in numerous studies [6–10] because of their compositional similarity to bone mineral, which results in desirable properties like biocompatibility, osteoconductivity, and bioactivity [11]. However, these materials are inherently brittle and are slowly resorbed [8].

An alternative to calcium phosphate ceramics is calcium phosphate cements. Calcium phosphate cements are prepared by mixing calcium phosphate powder with a liquid component to initiate an acid-base driven dissolution-precipitation reaction [12]. This process gives calcium phosphate cements several key advantages. In contrast to calcium phosphate ceramics, calcium phosphate cement microstructure consists of micron-sized crystals, which results in enhanced resorbability compared to sintered ceramics [13]. Highly resorbable calcium phosphate cements consisting of dicalcium phosphate dihydrate (DCPD) have the potential to degrade and be replaced by host bone [14,15], which is a key objective in bone tissue engineering. Perhaps the most important advantage of calcium phosphate cements, however, is their paste-like consistency prior to setting, which makes these biomaterials both injectable and moldable [16,17]. While this property is advantageous for filling irregularly shaped bone defects, it can also be leveraged for scaffold fabrication. Notably, it is possible to fabricate scaffolds with precisely controlled 3D architectures by indirect casting, which is a lost mold technique based on rapid prototyping technology [18]. This technique is highly advantageous because parameters such as pore size, location, and interconnectivity can be precisely controlled according to the CAD model used for mold fabrication [19,20].

The major disadvantage of calcium phosphate cements is their mechanical properties, as they are weaker than ceramics and are also brittle [21]. However, these disadvantages can be mitigated through polymer reinforcement [22–24]. We recently developed a polymer reinforcement method that is suitable for the fabrication of reinforced 3D calcium phosphate cement scaffolds [25]. Our method, which we have termed polymer infiltration and *in situ* curing, exploits the microporous nature of calcium phosphate cements by filling the micropores of a pre-set calcium phosphate cement structure with a polymer and then cross-linking the polymer *in situ*. We demonstrated proof of concept for our approach using a model polymer and showed substantial improvements in mechanical properties [25]. In the present study, we have sought to extend our work by developing a resorbable polymer reinforced DCPD composite with mechanical properties suitable for bone tissue engineering. To this end, we chose to use poly(propylene fumarate) (PPF), which is an unsaturated polyester, as the reinforcing polymer. PPF-based composites have been used extensively in bone tissue engineering and have shown good mechanical properties, biocompatibility, and osteoconductivity [26–29].

The objectives of this study were to manufacture and characterize PPF reinforced DCPD composites and evaluate their suitability for use as bone tissue engineering scaffold materials. To this end, we thoroughly characterized the mechanical properties of PPF-DCPD composites. In addition, we demonstrated the robustness of our approach by fabricating 3D scaffolds of various geometries. Finally, as a first step towards evaluating these composites for *in vivo* use, we used 3D PPF-DCPD scaffolds as part of a bone tissue engineering strategy to repair a calvarial defect in an animal model.

## MATERIALS AND METHODS

### Composite Preparation

DCPD cement was prepared using an equimolar mixture of monocalcium phosphate monohydrate (MCPM; Strem Chemicals, Newburyport, MA, USA) and  $\beta$ -tricalcium phosphate ( $\beta$ -TCP; Fluka Chemical Corporation, Ronkonkoma, NY). Deionized water was

used as the mixing liquid. The exact powder to liquid mass ratios (P/L) used for cement preparation, which varied according to the experiments, are given in subsequent sections. After allowing at least 30 minutes for the cements to fully set, the cements were placed in a vacuum desiccator chamber at room temperature for drying.

To reinforce the DCPD cement, a solution of PPF with cross-linking monomer and initiator was prepared. Briefly, PPF ( $M_p = 1,700$  g/mol; Scientific Polymer Products, Ontario, NY) was mixed with N-vinyl pyrrolidinone (NVP; Acros Organics, Geel, Belgium) in a 4:3 mass ratio. Butylated hydroxytoluene inhibitor (Acros Organics) was added to the solution at 0.1 wt % in order to prevent premature curing, and 5 wt % benzoyl peroxide (Acros Organics) was added as the free radical initiator. Fully dried DCPD cements were submerged in this PPF/NVP solution and placed in a vacuum chamber for 3 min to encourage polymer infiltration into the cement micropores. The specimens were subsequently removed, blotted dry to remove excess polymer, and then cured under vacuum at 80°C for 24 h.

### Evaluation of Composite Mechanical Properties

Bar-shaped cement specimens (2 mm × 2 mm × 25 mm) were prepared by casting unhardened DCPD cement paste into a stainless steel mold. P/L of 1.0 and 1.5 were used. Mechanical properties of PPF reinforced and non-reinforced control specimens were evaluated using a three point bending test. Testing was performed on an electromechanical materials testing machine equipped with a 125 N load cell (MTS Systems, Eden Prairie, MN), using a 15 mm span and 1 mm/min loading rate. Flexural strength, flexural modulus, maximum displacement, and work of fracture were calculated. Trends were correlated to the amount of polymer incorporation, which was determined by weighing the specimens before and after reinforcement.

### Cytocompatibility Assay

A stainless steel mold was used to prepare disks (15 mm diameter, 2 mm thickness) of DCPD cement with a P/L of 1.0. Following PPF reinforcement, the disks were rinsed in acetone for 3 minutes, rinsed with phosphate buffered saline (PBS), and then sterilized by soaking in 70% ethanol for 30 minutes. The disks were subsequently soaked in sterile PBS at 10 ml/disk for 7 days to leach out unreacted monomer.

Cytocompatibility of the PPF-DCPD composites was evaluated with a flow cytometry based assay, similar to what we previously described [30]. Briefly, murine mesenchymal stem cells (MSCs; see [31] for isolation and characterization) were plated at 100,000 cells/well in a 12 well plate. After the cells had attached, they were cultured for 24 h in media (Dulbecco's modified eagles medium, high glucose with 10% fetal bovine serum (Atlanta Biologicals, Lawrenceville, GA), 4 mM L-glutamine, 0.25 µg/ml amphotericin B, 100 IU/ml penicillin-G, and 100 µg/ml streptomycin (all from Invitrogen)) that had been conditioned by soaking a PPF-DCPD disk for 24 hours. Each disk was soaked in 3 ml of media. After 24 h, the media from each well was collected in order to include any detached cells in the analysis. The attached cells were then trypsinized, combined with the collected media, labeled with fluorescein isothiocyanate conjugated Annexin V (BD Biosciences; San Diego, CA) and 10 µg/ml propidium iodide (Sigma-Aldrich) to stain apoptotic and necrotic cells, respectively, and then analyzed on a FACSCaliber instrument (BD Biosciences) set to record 10,000 events. This method allows for the determination of the percent of viable cells in the population, which are unlabeled, as well as the percent of cells that are necrotic and apoptotic [32]. Gates for the analysis were established based on controls (i.e. cells exposed to 2 µg/ml saponin detergent to disrupt the cell membrane, and cells cultured in fresh medium).

### 3D Scaffold Fabrication and Characterization

3D DCPD scaffolds comprised of orthogonally intersecting beams were prepared by indirect casting, as we previously described [25]. Briefly, 3D models for the scaffolds were prepared using commercially available CAD software (Rhinoceros, McNeel North America, Seattle, WA). Negative wax molds were then printed on a Solidscape T66 benchtop rapid prototyping machine (Solidscape, Merrimack, NH) and subsequently used to cast DCPD scaffolds.

To demonstrate the versatility of our approach, three different scaffold designs were prepared. First, cylindrical scaffolds (8 mm diameter  $\times$  8.5 mm height) with 1 mm diameter beams spaced 750  $\mu$ m apart were prepared for compressive testing, as in our previous study [25]. Second, a smaller cylinder (4 mm diameter, 5 mm height) with a rectangular through-hole (1.75 mm  $\times$  1.75 mm) and 750  $\mu$ m diameter beams spaced 500  $\mu$ m apart was prepared to demonstrate the fabrication of smaller feature sizes. Finally, disk shaped scaffolds (9 mm diameter  $\times$  3 mm height) consisting of 1 mm diameter beams spaced 750  $\mu$ m apart in the x-y direction and 500  $\mu$ m in the z direction were prepared for evaluation in a rabbit calvarial defect model. All three scaffold designs were manufactured from DCPD cement prepared with a P/L ratio of 1.0 and then reinforced as described above. For microstructural evaluation, the reinforced scaffolds were imaged on a Jeol JSM-5310LV scanning electron microscope (SEM; Jeol, Tokyo, Japan) operating in low vacuum mode at an accelerating voltage of 15 kV. The scaffolds were not coated prior to imaging. To evaluate reinforced scaffold mechanical properties, the 8 mm diameter scaffolds were tested in compression on an electromechanical materials testing machine equipped with a 5 kN load cell using a 1 mm/min loading rate.

### *In Vivo* Study

*In vivo* evaluation of the 3D PPF reinforced DCPD scaffolds was performed under a protocol approved by the Institutional Animal Care and Use Committee of the Indiana University School of Dentistry. A total of 8 male New Zealand White rabbits weighing approximately 4 kg were used. Each animal received a scaffold seeded with bone marrow derived mesenchymal stem cells and a control scaffold with no cells. Prior to cell seeding, the PPF-DCPD scaffolds were sterilized by soaking in 70% ethanol for 30 min and then soaked in sterile PBS for 1 week. To seed the scaffolds with MSC, sterile filtered type I collagen gel derived from porcine skin was used as the cell carrier, as described by Kreger et al. [33]. MSC were suspended in the collagen at  $10^6$  cells/ml, and scaffolds were loaded with 150  $\mu$ l of the MSC/gel suspension. Collagen gel without cells was used as the control. Consistent with the experimental design, adult male New Zealand White rabbits approximately 4–5 months in age and weighing 4 kg served as the cell donors. Briefly, MSC were isolated from the femoral bone marrow based on adherence to plastic, similar to what we previously described [34]. To verify osteogenic differentiation prior to implantation, isolated cells were cultured for two weeks in media supplemented with dexamethasone,  $\beta$ -glycerophosphate, and ascorbic acid and stained for alkaline phosphatase (data not shown).

To prepare the animals for surgery, general anesthesia was given by an intramuscular ketamine injection (35 mg/kg). The scalps were shaved and cleaned. A sagittal incision was then made over the scalp. After subperiosteal undermining, two 10 mm diameter circular bone defects were made symmetrically in the parietal bones using a dental trephine bur. After the scaffolds were placed into the defects, the periosteum and scalp were closed with resorbable Vicryl sutures. Buprinorphine analgesic was given subcutaneously every 8–12 hours for pain management (0.02–0.05 mg/kg). One animal died during surgery, and another died the day after surgery. The remaining 6 animals encountered no complications and were humanely sacrificed after 6 weeks.

Excised calvarial specimens were fixed in 10 % neutral buffered formalin for one week and then analyzed by micro-computed tomography ( $\mu$ CT) on a  $\mu$ CT 20 workstation (Scanco Medical, Bruttisellen, Switzerland) operating at 50 kV and 160  $\mu$ A with a 100 ms integration time, resulting in a 34  $\mu$ m voxel size. Contours were drawn on sagittal image slices manually to define the volume of interest for 3D analysis around the scaffold. The 3D volume was reconstructed using a global threshold, which was adjusted in order to include both the scaffold and bone. The total volume of thresholded material was calculated. Following  $\mu$ CT analysis, the specimens were embedded un-decalcified in polymethyl methacrylate blocks for histological analysis. Three series of 4  $\mu$ m thin coronal sections were collected, starting at the center of the scaffold and then moving posteriorly in 1 mm increments. Thus, in the results section, series one was taken from the center of the scaffold, series two was taken 1 mm out from the center, and series three was taken 2 mm out from the center. Tissue sections were stained with von Kossa's method with a MacNeal's tetrachrome counterstain. Two sections from each series were analyzed at 100X magnification with Bioquant Osteo software (Bioquant Image Analysis Corporation, Nashville, TN) to quantify the percent of available space within the defect that was occupied by new bone.

### Statistical Analysis

All quantitative data are presented as the mean plus or minus the standard deviation. Statistical analysis was performed using SAS version 9.2 (SAS Institute Inc., Cary, NC;  $\alpha = 0.05$  for all experiments). The effects of P/L and reinforcement on the composite mechanical properties (i.e. flexural strength, modulus, etc.) were evaluated using an ANOVA mixed effects model. The percents of viable, necrotic and apoptotic cells measured in the cytocompatibility assay were compared with a t-test. The compressive strengths of reinforced and non-reinforced 3D scaffolds were compared using a non-parametric t-test. For the *in vivo* study, the effect of the MSC treatment versus the control on the thresholded tissue/scaffold volume measured by  $\mu$ CT was evaluated using a paired t-test. Similarly, the effect of MSCs on the total percent of available area occupied by bone measured by histomorphometry was also evaluated by a paired t-test. Finally, the effects of MSC and series number on the percent of available area occupied by bone in the different regions of the scaffold measured by histomorphometry was evaluated using an ANOVA mixed effects model with animal number being included as a blocking factor. Where appropriate, multiple comparisons were performed using Tukey's method.

## RESULTS

### Effect of Polymer Reinforcement on Mechanical Properties

As expected, cement P/L had a significant effect on polymer incorporation, with polymer incorporation being increased at lower P/L (Figure 1A). At P/L of 1.0, polymer incorporation was  $0.38 \pm 0.02$  mg/mm<sup>3</sup>, whereas cements prepared with a P/L of 1.5 had a polymer incorporation of  $0.20 \pm 0.02$  mg/mm<sup>3</sup> ( $p < 0.05$ ).

P/L and polymer reinforcement both had a significant effect on the flexural strength of the DCPD cements (Figure 1B). The non-reinforced controls had a flexural strength of  $1.80 \pm 0.19$  MPa at P/L of 1.0, whereas PPF reinforcement improved the flexural strength to  $16.14 \pm 1.70$  MPa ( $p < 0.05$ ). In contrast, at P/L of 1.5 the non-reinforced controls had a flexural strength of  $6.54 \pm 1.34$  MPa, while the PPF reinforced group had a flexural strength of  $7.52 \pm 1.54$ . This difference was not statistically significant.

P/L also had a significant effect on flexural modulus (Figure 1C). At P/L of 1.0, the non-reinforced cements had a flexural modulus of  $1073.01 \pm 158.40$  MPa. The modulus of the

reinforced cements was slightly increased to  $1303.91 \pm 110.41$  MPa ( $p < 0.05$ ). At P/L of 1.5, the non-reinforced controls had a flexural modulus of  $2722.87 \pm 268.34$  MPa ( $p < 0.05$  for all comparisons). However, the modulus of the reinforced group at P/L of 1.5 was significantly reduced to  $1312.31 \pm 200.20$  MPa. The difference between the reinforced groups was not statistically significant.

As expected, the non-reinforced controls were very brittle and failed at low displacements during the three point bending test (Figure 1D). The non-reinforced DCPD cements failed at  $0.11 \pm 0.04$  mm and  $0.12 \pm 0.05$  mm at P/L of 1.0 and 1.5, respectively. PPF reinforcement resulted in significant increases to  $0.51 \pm 0.09$  mm and  $0.29 \pm 0.11$  mm ( $p < 0.05$ ) at P/L of 1.0 and 1.5, respectively.

Work of fracture was calculated as the area under the force- displacement curves normalized to cross-sectional area of the specimen, (Figure 1E). Due to their low strength and brittleness, non-reinforced cements absorbed very little energy before failing. The work of fracture for non-reinforced controls was  $2.74 \pm 0.78$  J/m<sup>2</sup> and  $13.74 \pm 3.73$  J/m<sup>2</sup> at P/L of 1.0 and 1.5, respectively. The increased strength and ductility of the PPF reinforced groups led to significant increases in work of fracture values. As expected, the largest increases were seen at P/L of 1.0. Reinforced cements at P/L of 1.0 had a work of fracture of  $249.21 \pm 81.64$  J/m<sup>2</sup> ( $p < 0.05$ ). Smaller increases were seen at P/L of 1.5. The reinforced cements had a work of fracture of  $83.78 \pm 29.24$  J/m<sup>2</sup>, which was not significantly different from the non-reinforced controls.

### Cytocompatibility of PPF reinforced DCPD

Cytocompatibility of PPF reinforced DCPD composites was evaluated by quantifying cell viability using a flow cytometry based assay.  $96.00 \pm 0.19$  percent of the cells exposed to medium conditioned with PPF-DCPD that was pre-soaked in PBS for 7 days were negative for both annexin V and propidium iodide, indicative of excellent cell viability. There were no significant differences in the percentages of the cells that were viable, necrotic, early apoptotic, and dead by apoptosis compared to the negative control (Figure 2, Table 1).

### 3D Scaffold Reinforcement

The robustness of our approach for fabricating resorbable 3D PPF reinforced DCPD cement scaffolds for bone tissue engineering was demonstrated using three different scaffold designs. While all of the scaffolds consisted of orthogonally intersecting beams, which is an ideal structure for promoting bone ingrowth [35], the overall geometry of the scaffolds and their feature sizes were varied (Figure 3A–C). The first scaffold design, which is identical to one we have previously used [25], was a large cylinder suitable for mechanical testing. The second was a smaller cylinder with a through hole, which mimics the geometry of a long bone. However, this design consisted of smaller feature sizes than the other two. Finally, the third was a disk geometry, which was designed for use in our rabbit cavariar defect study. Electron microscopy images of the reinforced scaffolds showed that the final products corresponded well with the CAD designs (Figure 3D–F). Furthermore, plate-like crystals, which are characteristic of DCPD [36], were still visible after PPF reinforcement when the samples were imaged at high magnification (Figure 3G). Given that the formation of a polymer shell around the outside of the cement would occlude the view of DCPD crystals from the surface, this observation suggests that the polymer infiltrated the cement micropores. This result is consistent with what we previously observed for cement reinforcement by polymer infiltration and *in situ* curing using poly(ethylene glycol) diacrylate as a model polymer [25].

Compressive testing of the cylindrical scaffolds showed that the effects of PPF reinforcement on DCPD mechanical properties translated to excellent scaffold mechanical properties (Figure 4). As expected, non-reinforced scaffolds failed at low loads and strains, and had an average compressive strength  $0.31 \pm 0.06$  MPa. In contrast, PPF reinforcement resulted in both increased strength and ductility. The stress-strain curves of the PPF-DCPD composite scaffolds showed distinct peaks and dips corresponding to yielding prior to catastrophic failure. The ultimate compressive strength of the PPF reinforced scaffolds was significantly increased to  $7.48 \pm 0.77$  MPa ( $p < 0.05$ ).

### **In Vivo Study**

Disk-shaped PPF-DCPD composite scaffolds with and without MSCs were implanted into bilateral parietal defects in rabbits for 6 weeks (Figure 5). Although a mild foreign body reaction to the scaffold was observed, the materials were generally well tolerated by the animals and no fibrous tissue encapsulation was encountered. The scaffold was easily distinguished histologically due to its unique staining characteristics. Importantly, several large nodules of woven bone with active osteoblasts lining the surfaces were observed within the scaffold pores (Figure 6), especially in the peripheral regions but also occasionally in the center of the defect. The scaffolds were clearly distinguished from bone by  $\mu$ CT due to their lower mineral density (Figure 7A). The thresholded volume within the defect (i.e. new bone + scaffold) was calculated to be  $113.31 \pm 22.87$  mm<sup>3</sup> and  $127.00 \pm 17.32$  mm<sup>3</sup> for MSC seeded and control scaffolds, respectively ( $n = 6$ ; Figure 7B), which was not a statistically significant difference. Quantitative histomorphometric measurements (Figure 7C) showed that the percent of available area filled with bone was only about 10–15 %. Analysis of different regions showed that the percent fills were  $6.40 \pm 2.22$  %,  $8.89 \pm 4.24$  %, and  $15.88 \pm 12.53$  % for the MSC seeded scaffolds and  $10.34 \pm 4.47$  %,  $13.81 \pm 7.84$  %, and  $25.44 \pm 16.49$  % for the control scaffolds at series one, two and three, respectively ( $n = 4$  for the MSC group at series one;  $n = 5$  for the MSC group at series two and the control group at series one;  $n = 6$  for all others). The effect of series number was significant by ANOVA, with the percent of area filled with bone being significantly higher for series three than for series one ( $p < 0.05$ ).

## **DISCUSSION**

Due to the ability to combine advantages and mitigate limitations of individual materials, composites are becoming increasingly important as biomaterials for bone repair. In this study we describe a novel calcium phosphate cement based composite scaffold material for bone tissue engineering. Calcium phosphate cements possess many desirable properties for bone tissue engineering scaffolds, including biocompatibility, resorbability, osteoconductivity, injectability, and moldability [11,13–15,37]. Nevertheless, low strength and brittleness have limited the applicability of calcium phosphate cements as scaffold materials. The mechanical properties limitations of non-reinforced calcium phosphate cements are clear throughout our data, as the non-reinforced controls were very weak (flexural strength  $< 2$  MPa at P/L = 1.0) and brittle (work of fracture  $\sim 2.75$  J/m<sup>2</sup> at P/L = 1.0).

Considering both the advantages and disadvantages of calcium phosphate cements, a composites approach to the fabrication of calcium phosphate cement based scaffolds for bone tissue engineering is clearly desirable. Due to the known logarithmic relationship between porosity and strength, we hypothesized that calcium phosphate cements can be effectively reinforced by filling void space with a polymeric component. In a previous study we tested this hypothesis and demonstrated proof of concept for manufacturing 3D polymer reinforced calcium phosphate cement scaffolds by a method, which we have termed polymer infiltration and *in situ* curing, using poly(ethylene glycol) diacrylate as a model reinforcing

polymer [25]. Importantly, unlike previously proposed methods of cement reinforcement [22,24,38,39], our method does not rely on the incorporation of fibers or polymeric additives to the cement, which may be prohibitive to 3D scaffold manufacturing. In the present study we have reinforced DCPD cement with cross-linked PPF. DCPD cement is highly resorbable because it is a metastable phase at physiologic pH [40]. However, DCPD cement is also very weak, even weaker than apatite forming calcium phosphate cements [41], and 3D scaffolds of pure DCPD would easily crumble *in vivo* due to a lack of mechanical integrity.

We chose to use PPF as a reinforcing polymer for several reasons. First, PPF is hydrolytically degradable, and its degradation products (i.e. fumaric acid and propylene glycol) are non-cytotoxic in low doses [42]. Second, PPF contains a double bond in its repeating unit, giving it numerous potential crosslinking sites along the polymer backbone. As a result, PPF can be cured *in situ*, making it ideal for our approach to calcium phosphate cement scaffold reinforcement. Finally, PPF based composites containing various calcium phosphate fillers have been studied extensively for bone tissue engineering applications. Notably, strengths exceeding trabecular bone have been reported [43,44], and excellent osteoconductivity has been noted in multiple studies [45,46]. Furthermore, histological results from *in vivo* studies have shown good biocompatibility of the PPF-based composites [45,47], although Peter et al. did note a mild inflammatory response [27]. It should be noted, however, that our PPF-DCPD composites are fundamentally different from previously published PPF/calcium phosphate composites. In all of the prior approaches, calcium phosphate particles have been dispersed within a crosslinked PPF matrix. In contrast, in our approach the crosslinked PPF fills the micropores of a cementitious matrix, resulting in a distinctly different microstructure. Interestingly, our method also results in a lower weight percent of polymer in the composite. For example, the PPF/ $\beta$ -tricalcium phosphate composites we used in a previous study contained approximately 73 wt % polymer [45], whereas the PPF-DCPD cement composites in this study contained a maximum of 28 wt % polymer (data not shown). Given the slow rate of PPF hydrolysis, this difference will likely facilitate faster biodegradation in long-term studies.

To characterize the mechanical properties of our novel PPF-DCPD composites, we chose to vary the DCPD cement P/L in order to determine the effects of this variable on the composite mechanical properties. Cement P/L is the primary determinant of cement microporosity, and, as shown in our prior study, this variable ultimately controls the extent of polymer incorporation. As expected, we found that increasing the cement P/L reduced the amount of polymer incorporation (Figure 1A). Cements prepared with P/L of 1.0 incorporated  $0.38 \pm 0.02 \text{ mg/mm}^3$  of the PPF/NVP mixture, whereas cements prepared with a P/L of 1.5 incorporated only  $0.20 \pm 0.02 \text{ mg/mm}^3$ . Interestingly, these values are lower than what we measured in our previous study due to the high viscosity of the non-crosslinked PPF solution ( $\sim 6,700 \text{ mPa}\cdot\text{s}$ ). Nevertheless, PPF reinforcement led to significant improvements in mechanical properties (Figure 1B-FE). Only modest improvements were observed for the cements prepared with P/L of 1.5 due to the lower amount of polymer incorporation. However, at P/L of 1.0 flexural strength was improved from  $1.80 \pm 0.19 \text{ MPa}$  to  $16.14 \pm 1.70 \text{ MPa}$ , modulus increased from  $1073.01 \pm 158.40 \text{ MPa}$  to  $1303.91 \pm 110.41 \text{ MPa}$ , maximum displacement increased from  $0.11 \pm 0.04 \text{ mm}$  to  $0.51 \pm 0.09 \text{ mm}$ , and work of fracture increased from  $2.74 \pm 0.78 \text{ J/m}^2$  to  $249.21 \pm 81.64 \text{ J/m}^2$  ( $p < 0.05$  for all comparisons).

Calcium phosphate cement reinforcement by polymer infiltration and *in situ* curing is compatible with 3D scaffold fabrication because the reinforcing polymer is incorporated into a pre-set cement structure [25]. Theoretically any 3D cement structure which can be manufactured, either by our method or by other methods like 3D powder printing [48], could

be reinforced. This is an important advantage considering the possibility of using medical imaging data to design customized, patient-specific scaffolds [19]. To illustrate the versatility of our methodology, in this study we manufactured three different 3D macroporous PPF-DCPD scaffolds. All three scaffolds were comprised of orthogonally intersecting cylindrical beams, but differed in the beam size and spacing, as well as the macroscale geometry. In all cases the scaffold pores were free of polymer and the DCPD crystalline microstructure could be visualized by SEM, indicating that the polymer infiltrated the cement. Although further studies are needed to determine the lower limit of size features which can be attained, PPF reinforcement does not appear to affect the macroscopic scaffold architecture. Importantly, all of the PPF-DCPD scaffolds had good mechanical integrity compared to non-reinforced controls. Non-reinforced 3D scaffolds subjected to compressive testing had a strength of only  $0.31 \pm 0.06$  MPa. PPF reinforcement increased the scaffold compressive strength more than 20 fold to  $7.48 \pm 0.77$  MPa (Figure 4;  $p < 0.05$ ). Importantly, this value is comparable to the compressive strength of trabecular bone [43] demonstrating that 3D PPF reinforced DCPD scaffolds have suitable mechanical properties for bone tissue engineering.

Finally, to evaluate PPF-DCPD composites for bone tissue engineering applications, the disk shaped 3D scaffolds were seeded with MSC and implanted into calvarial defects in rabbits. The addition of MSCs was not found to increase the amount of bone formation in this study (Figure 7). Similar results were reported by Schantz et al., who also saw very little bone formation (4.7%) at 3 months when scaffolds were seeded with rabbit MSCs and used to repair rabbit calvarial defects [49]. Nevertheless, this result was somewhat surprising. At this time, the exact reason is unclear. It is possible that the cell seeding density of 150,000 cells per scaffold was too low, and there were simply not enough viable cells after implantation to significantly improve bone regeneration. Future studies should investigate the effect of seeding density, as well as methods to improve scaffold seeding, induce osteogenic differentiation, and track the fate of implanted MSCs.

Since MSCs did not have a significant effect, bone formation in the 3D PPF-DCPD scaffolds appeared to be due primarily to tissue ingrowth from the surrounding calvarial bone. This conclusion is supported by the fact that the effect of series number was significant in the two way ANOVA analysis of the histomorphometry data, with significantly more bone present closer to the edges of the defect (i.e. in series 3;  $p < 0.05$ ). Although the overall extent of bone formation that we observed was relatively low, it is worth noting that we only evaluated bone formation at 6 weeks. It is likely that at later time points bone ingrowth into our 3D PPF reinforced DCPD scaffolds would be increased. In a similar experimental model, Dean et al. showed significant increases in calvarial bone formation from 6 weeks to 12 weeks [50].

Importantly, none of the implanted 3D scaffolds showed evidence of mechanical failure, which would not have been possible without PPF reinforcement. Qualitative analysis of tissue sections revealed that there were numerous nodules of woven bone lined with active osteoblasts (Figure 6). Direct apposition of bone onto the scaffold was not observed, but new bone was frequently observed by both  $\mu$ CT and histology to form an interpenetrating network within the scaffold. In some cases the percent of available area filled with bone measured by histomorphometry was as high as 50 %. Overall, these results suggest that PPF-DCPD cement composites can provide a good scaffold for bone regeneration.

## CONCLUSIONS

This study introduces novel PPF-DCPD composites as scaffold materials for bone tissue engineering. Applying our novel method of polymer infiltration and *in situ* curing for

calcium phosphate cement reinforcement, we demonstrated the effective reinforcement of DCPD cement with PPF. Characterization of mechanical properties revealed that the amount of polymer incorporation determined the reinforcement efficacy, with higher amounts being more effective. Furthermore, the excellent mechanical properties achieved were shown to translate to 3D scaffold fabrication, as PPF reinforced DCPD cement scaffolds were comparable to trabecular bone in compressive strength. Finally, *in vivo* evaluation in a rabbit calvarial defect model showed that, although the addition of MSCs did not enhance tissue regeneration, bone was able to grow into the pores of PPF-DCPD cement scaffolds from the surrounding bone tissue. Collectively, the data indicate that PPF reinforced DCPD cement composites are a potentially useful material platform for bone tissue engineering.

## Acknowledgments

The authors thank Ms. Meaghan MacPherson and Mr. Clif Dunh for their assistance with the mechanical testing and SEM imaging of the PPF-DCPD composites. We also thank, Ms. Dan Zhou for her assistance with the MSC isolation and culture, Dr. Alex Robling for the use of the  $\mu$ CT instrument and for his assistance with the analysis, and Dr. Keith Condon for his assistance with the histology. This work was supported in part by National Institutes of Health grant K08 HL75253 (WSG) and by Indiana University School of Dentistry Professional Development Fund (TGC). WSG is Medical Director for General BioTechnology, LLC; The Genesis Bank, LLC; and Renovocyte, LLC.

## References

1. Chatterjea A, Meijer G, van Blitterswijk C, de Boer J. Clinical application of human mesenchymal stromal cells for bone tissue engineering. *Stem Cells Int.* 2010; 2010:215625. [PubMed: 21113294]
2. Mesimäki K, Lindroos B, Törnwall J, Mauno J, Lindqvist C, Kontio R, et al. Novel maxillary reconstruction with ectopic bone formation by GMP adipose stem cells. *Int J Oral Maxillofac Surg.* 2009 Mar; 38(3):201–209. [PubMed: 19168327]
3. Quarto R, Mastrogiacomo M, Cancedda R, Kutepov SM, Mukhachev V, Lavroukov A, et al. Repair of large bone defects with the use of autologous bone marrow stromal cells. *N Engl J Med.* 2001 Feb 1; 344(5):385–386. [PubMed: 11195802]
4. Marcacci M, Kon E, Moukhachev V, Lavroukov A, Kutepov S, Quarto R, et al. Stem cells associated with macroporous bioceramics for long bone repair: 6- to 7-year outcome of a pilot clinical study. *Tissue Eng.* 2007 May; 13(5):947–955. [PubMed: 17484701]
5. Morishita T, Honoki K, Ohgushi H, Kotobuki N, Matsushima A, Takakura Y. Tissue engineering approach to the treatment of bone tumors: three cases of cultured bone grafts derived from patients mesenchymal stem cells. *Artif Organs.* 2006 Feb; 30(2):115–118. [PubMed: 16433845]
6. Arinze TL, Peter SJ, Archambault MP, van den Bos C, Gordon S, Kraus K, et al. Allogeneic mesenchymal stem cells regenerate bone in a critical-sized canine segmental defect. *J Bone Joint Surg Am.* 2003 Oct; 85-A(10):1927–1935. [PubMed: 14563800]
7. Arinze TL, Tran T, Mcalary J, Daculsi G. A comparative study of biphasic calcium phosphate ceramics for human mesenchymal stem-cell-induced bone formation. *Biomaterials.* 2005 Jun; 26(17):3631–3638. [PubMed: 15621253]
8. Wagoner Johnson AJ, Herschler BA. A review of the mechanical behavior of CaP and CaP/polymer composites for applications in bone replacement and repair. *Acta Biomater.* 2011; 7(1):16–30. [PubMed: 20655397]
9. Liu G, Zhao L, Zhang W, Cui L, Liu W, Cao Y. Repair of goat tibial defects with bone marrow stromal cells and beta-tricalcium phosphate. *J Mater Sci Mater Med.* 2008 Jun; 19(6):2367–2376. [PubMed: 18158615]
10. Barrère F, van Blitterswijk CA, de Groot K. Bone regeneration: molecular and cellular interactions with calcium phosphate ceramics. *Int J Nanomedicine.* 2006; 1(3):317–332. [PubMed: 17717972]
11. LeGeros RZ. Properties of osteoconductive biomaterials: calcium phosphates. *Clin Orthop Relat Res.* 2002 Feb.(395):81–98. [PubMed: 11937868]

12. Ginebra MP, Espanol M, Montufar EB, Perez RA, Mestres G. New processing approaches in calcium phosphate cements and their applications in regenerative medicine. *Acta Biomater.* 2010 Aug; 6(8):2863–2873. [PubMed: 20123046]
13. Bohner M. Calcium orthophosphates in medicine: from ceramics to calcium phosphate cements. *Injury.* 2000 Dec; 31( Suppl 4):37–47. [PubMed: 11270080]
14. Theiss F, Apelt D, Brand B, Kutter A, Zlinszky K, Bohner M, et al. Biocompatibility and resorption of a brushite calcium phosphate cement. *Biomaterials.* 2005 Jul; 26(21):4383–4394. [PubMed: 15701367]
15. Apelt D, Theiss F, El-Warrak AO, Zlinszky K, Bettschart-Wolfisberger R, Bohner M, et al. In vivo behavior of three different injectable hydraulic calcium phosphate cements. *Biomaterials.* 2004 Apr; 25(7–8):1439–1451. [PubMed: 14643619]
16. Khairoun I, Boltong MG, Driessens FC, Planell JA. Some factors controlling the injectability of calcium phosphate bone cements. *J Mater Sci Mater Med.* 1998 Aug; 9(8):425–428. [PubMed: 15348854]
17. Low KL, Tan SH, Zein SHS, Roether JA, Mouriño V, Boccaccini AR. Calcium phosphate-based composites as injectable bone substitute materials. *J Biomed Mater Res Part B Appl Biomater.* 2010 Jul; 94(1):273–286. [PubMed: 20336722]
18. Chu TM, Halloran JW, Hollister SJ, Feinberg SE. Hydroxyapatite implants with designed internal architecture. *J Mater Sci Mater Med.* 2001 Jun; 12(6):471–478. [PubMed: 15348260]
19. Hollister SJ, Lin CY, Saito E, Lin CY, Schek RD, Taboas JM, et al. Engineering craniofacial scaffolds. *Orthod Craniofac Res.* 2005 Aug; 8(3):162–173. [PubMed: 16022718]
20. Mitsak AG, Kempainen JM, Harris MT, Hollister SJ. Effect of Polycaprolactone Scaffold Permeability on Bone Regeneration In Vivo. *Tissue Eng Part A.* 2011 Jul; 17(13–14):1831–9. [PubMed: 21395465]
21. Ambard AJ, Mueninghoff L. Calcium phosphate cement: review of mechanical and biological properties. *J Prosthodont.* 2006 Oct; 15(5):321–328. [PubMed: 16958734]
22. Gorst NJS, Perrie Y, Gbureck U, Hutton AL, Hofmann MP, Grover LM, et al. Effects of fibre reinforcement on the mechanical properties of brushite cement. *Acta Biomater.* 2006; 2(1):95–102. [PubMed: 16701863]
23. Zhang Y, Xu HHK. Effects of synergistic reinforcement and absorbable fiber strength on hydroxyapatite bone cement. *J Biomed Mater Res A.* 2005 Dec 15; 75(4):832–840. [PubMed: 16138342]
24. Xu HH, Eichmiller FC, Barndt PR. Effects of fiber length and volume fraction on the reinforcement of calcium phosphate cement. *J Mater Sci Mater Med.* 2001; 12(1):57–65. [PubMed: 15348378]
25. Alge DL, Chu T-MG. Calcium phosphate cement reinforcement by polymer infiltration and in situ curing: a method for 3D scaffold reinforcement. *J Biomed Mater Res A.* 2010 Aug; 94(2):547–555. [PubMed: 20186776]
26. Chang C-H, Liao T-C, Hsu Y-M, Fang H-W, Chen C-C, Lin F-H. A poly(propylene fumarate)--calcium phosphate based angiogenic injectable bone cement for femoral head osteonecrosis. *Biomaterials.* 2010 May; 31(14):4048–4055. [PubMed: 20172606]
27. Peter SJ, Miller ST, Zhu G, Yasko AW, Mikos AG. In vivo degradation of a poly(propylene fumarate)/beta-tricalcium phosphate injectable composite scaffold. *J Biomed Mater Res.* 1998 Jul; 41(1):1–7. [PubMed: 9641618]
28. Kim K, Dean D, Mikos AG, Fisher JP. Effect of initial cell seeding density on early osteogenic signal expression of rat bone marrow stromal cells cultured on cross-linked poly(propylene fumarate) disks. *Biomacromolecules.* 2009 Jul 13; 10(7):1810–1817. [PubMed: 19469498]
29. Lee K-W, Wang S, Yaszemski MJ, Lu L. Physical properties and cellular responses to crosslinkable poly(propylene fumarate)/hydroxyapatite nanocomposites. *Biomaterials.* 2008 Jul; 29(19):2839–2848. [PubMed: 18403013]
30. Alge DL, Goebel WS, Chu T-MG. In vitro degradation and cytocompatibility of dicalcium phosphate dihydrate cements prepared using the monocalcium phosphate monohydrate/hydroxyapatite system reveals rapid conversion to HA as a key mechanism. *J Biomed Mater Res Part B Appl Biomater.* In press.

31. Li Y, Chen S, Yuan J, Yang Y, Li J, Ma J, et al. Mesenchymal stem/progenitor cells promote the reconstitution of exogenous hematopoietic stem cells in Fancg<sup>-/-</sup> mice in vivo. *Blood*. 2009 Mar 5; 113(10):2342–51. [PubMed: 19129541]
32. Vermes I, Haanen C, Steffens-Nakken H, Reutelingsperger C. A novel assay for apoptosis. Flow cytometric detection of phosphatidylserine expression on early apoptotic cells using fluorescein labelled Annexin V. *J Immunol Methods*. 1995 Jul 17; 184(1):39–51. [PubMed: 7622868]
33. Kreger ST, Bell BJ, Bailey J, Stites E, Kuske J, Waisner B, et al. Polymerization and matrix physical properties as important design considerations for soluble collagen formulations. *Biopolymers*. 2010 Aug; 93(8):690–707. [PubMed: 20235198]
34. Alge DL, Zhou D, Adams LL, Wyss BK, Shadday MD, Woods EJ, et al. Donor-matched comparison of dental pulp stem cells and bone marrow-derived mesenchymal stem cells in a rat model. *J Tissue Eng Regen Med*. 2010; 4(1):73–81. [PubMed: 19842108]
35. Chu TMG, Orton DG, Hollister SJ, Feinberg SE, Halloran JW. Mechanical and in vivo performance of hydroxyapatite implants with controlled architectures. *Biomaterials*. 2002 Mar; 23(5):1283–1293. [PubMed: 11808536]
36. Alge DL, Santa Cruz G, Goebel WS, Chu T-MG. Characterization of dicalcium phosphate dihydrate cements prepared using a novel hydroxyapatite-based formulation. *Biomed Mater*. 2009 Apr.4(2):025016. [PubMed: 19349655]
37. Bohner M, Baroud G. Injectability of calcium phosphate pastes. *Biomaterials*. 2005 May; 26(13): 1553–1563. [PubMed: 15522757]
38. Chen W-C, Ju C-P, Wang J-C, Hung C-C, Chern Lin J-H. Brittle and ductile adjustable cement derived from calcium phosphate cement/polyacrylic acid composites. *Dent Mater*. 2008 Dec; 24(12):1616–1622. [PubMed: 18502499]
39. Xu HHK, Quinn JB, Takagi S, Chow LC. Processing and properties of strong and non-rigid calcium phosphate cement. *J Dent Res*. 2002 Mar; 81(3):219–224. [PubMed: 11881631]
40. Fernández E, Gil FJ, Ginebra MP, Driessens FC, Planell JA, Best SM. Calcium phosphate bone cements for clinical applications. Part I: solution chemistry. *J Mater Sci Mater Med*. 1999 Mar; 10(3):169–176. [PubMed: 15348165]
41. Charrière E, Terrazzoni S, Pittet C, Mordasini PH, Dutoit M, Lemaître J, et al. Mechanical characterization of brushite and hydroxyapatite cements. *Biomaterials*. 2001 Nov; 22(21):2937–2945. [PubMed: 11561900]
42. Timmer MD, Jo S, Wang C, Ambrose CG, Mikos AG. Characterization of the Cross-Linked Structure of Fumarate-Based Degradable Polymer Networks. *Macromolecules*. 2002; 35(11): 4373–4379.
43. Yaszemski MJ, Payne RG, Hayes WC, Langer R, Mikos AG. In vitro degradation of a poly(propylene fumarate)-based composite material. *Biomaterials*. 1996 Nov; 17(22):2127–2130. [PubMed: 9035745]
44. Wu C-C, Yang K-C, Yang S-H, Lin M-H, Kuo T-F, Lin F-H. In Vitro Studies of Composite Bone Filler Based on Poly(Propylene Fumarate) and Biphasic  $\alpha$ -Tricalcium Phosphate/Hydroxyapatite Ceramic Powder. *Artif Organs*. In press.
45. Chu T-MG, Warden SJ, Turner CH, Stewart RL. Segmental bone regeneration using a load-bearing biodegradable carrier of bone morphogenetic protein-2. *Biomaterials*. 2007; 28(3):459–467. [PubMed: 16996588]
46. Lewandrowski K-U, Bondre SP, Wise DL, Trantolo DJ. Enhanced bioactivity of a poly(propylene fumarate) bone graft substitute by augmentation with nano-hydroxyapatite. *Biomed Mater Eng*. 2003; 13(2):115–124. [PubMed: 12775902]
47. Cai Z, Zhang T, Di L, Xu D-M, Xu D-H, Yang D-A. Morphological and histological analysis on the in vivo degradation of poly (propylene fumarate)/(calcium sulfate/ $\beta$ -tricalcium phosphate). *Biomed Microdevices*. 2011 Aug; 13(4):623–31. [PubMed: 21448654]
48. Gbureck U, Hölzel T, Klammert U, Würzler K, Müller FA, Barralet JE. Resorbable Dicalcium Phosphate Bone Substitutes Prepared by 3D Powder Printing. *Adv Funct Mater*. 2007; 17(18): 3940–3945.

49. Schantz J-T, Hutmacher DW, Lam CXF, Brinkmann M, Wong KM, Lim TC, et al. Repair of calvarial defects with customised tissue-engineered bone grafts II. Evaluation of cellular efficiency and efficacy in vivo. *Tissue Eng.* 2003; 9( Suppl 1):S127–139. [PubMed: 14511476]
50. Dean D, Wolfe MS, Ahmad Y, Totonchi A, Chen JE-K, Fisher JP, et al. Effect of transforming growth factor beta 2 on marrow-infused foam poly(propylene fumarate) tissue-engineered constructs for the repair of critical-size cranial defects in rabbits. *Tissue Eng.* 2005 Jun; 11(5–6): 923–939. [PubMed: 15998232]

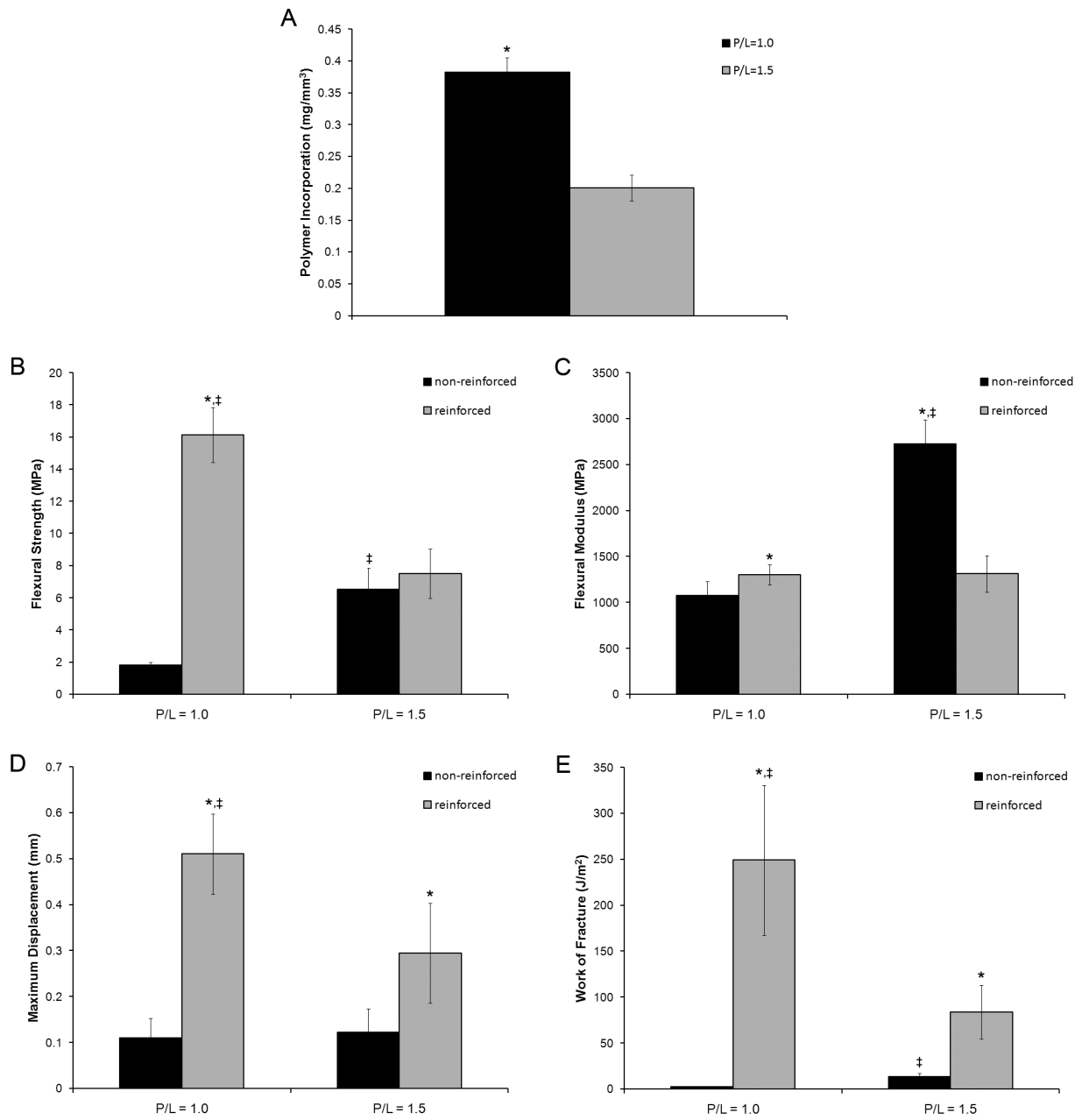


Figure 1.

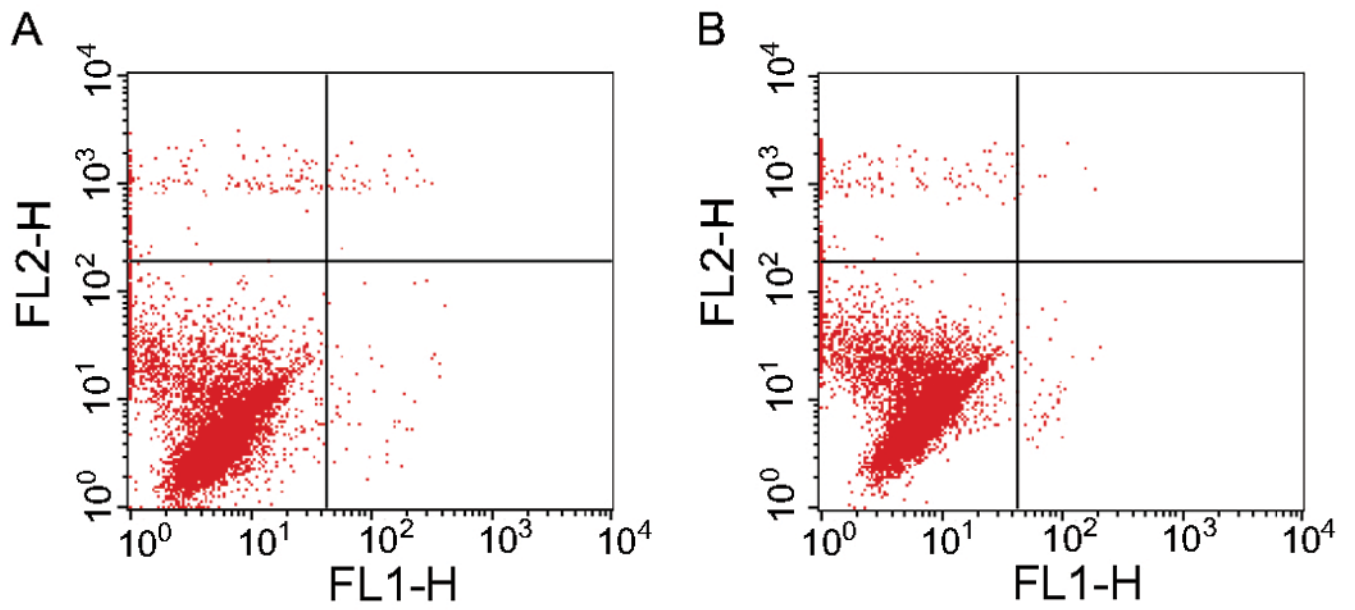


Figure 2.

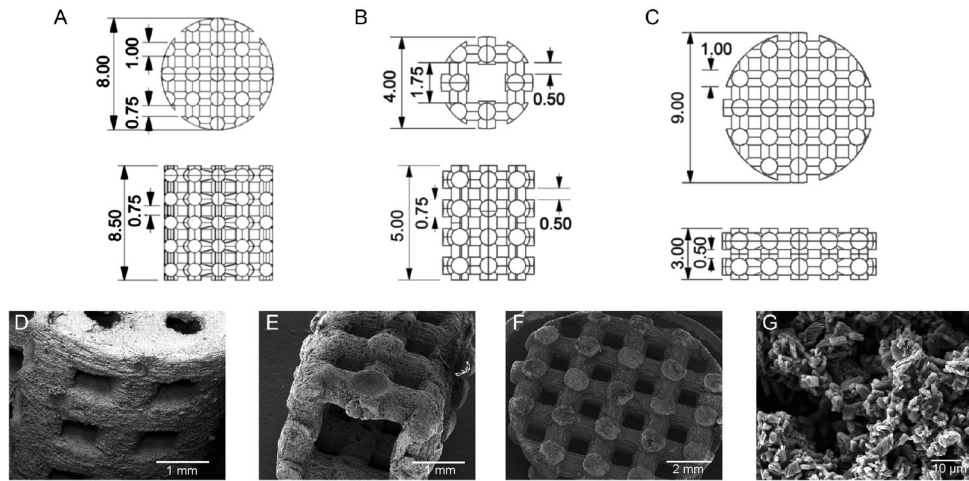


Figure 3.

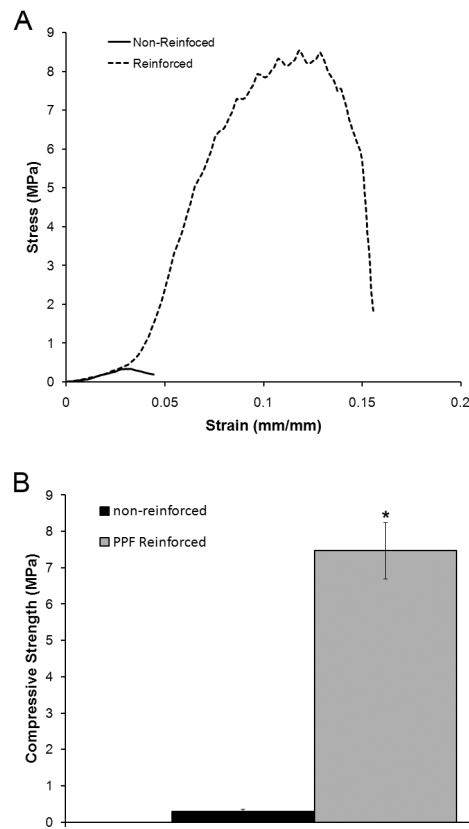
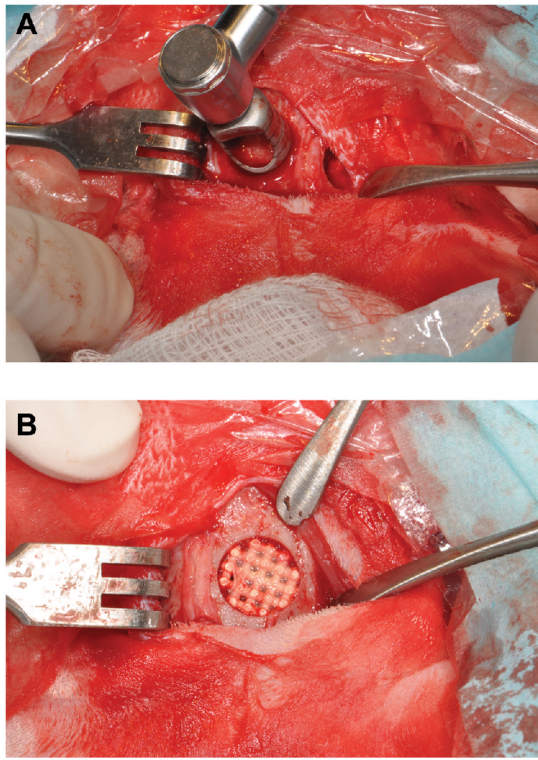


Figure 4.



**Figure 5.**

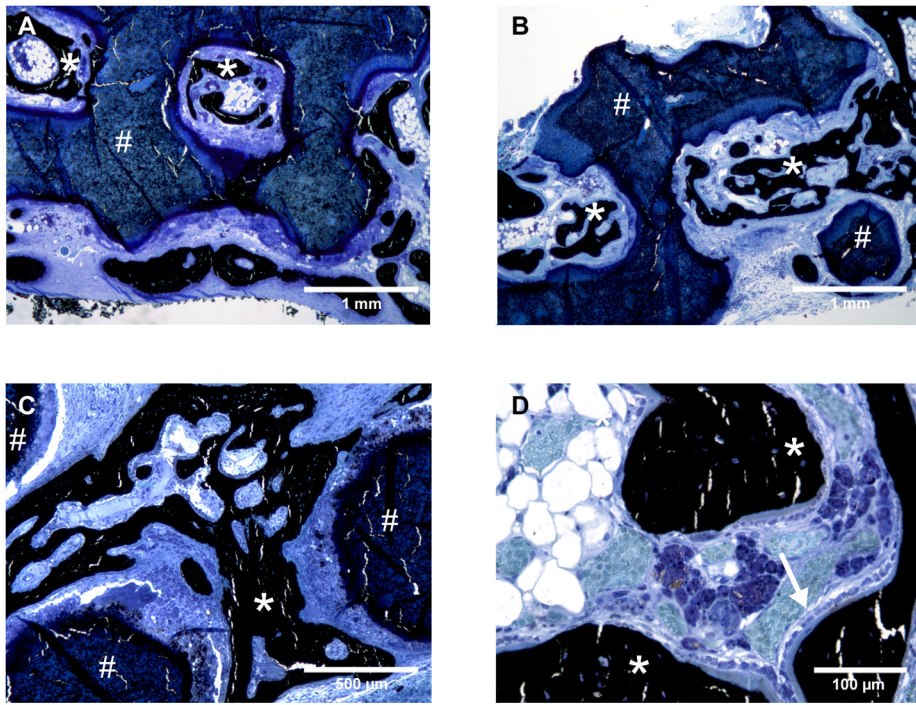


Figure 6.

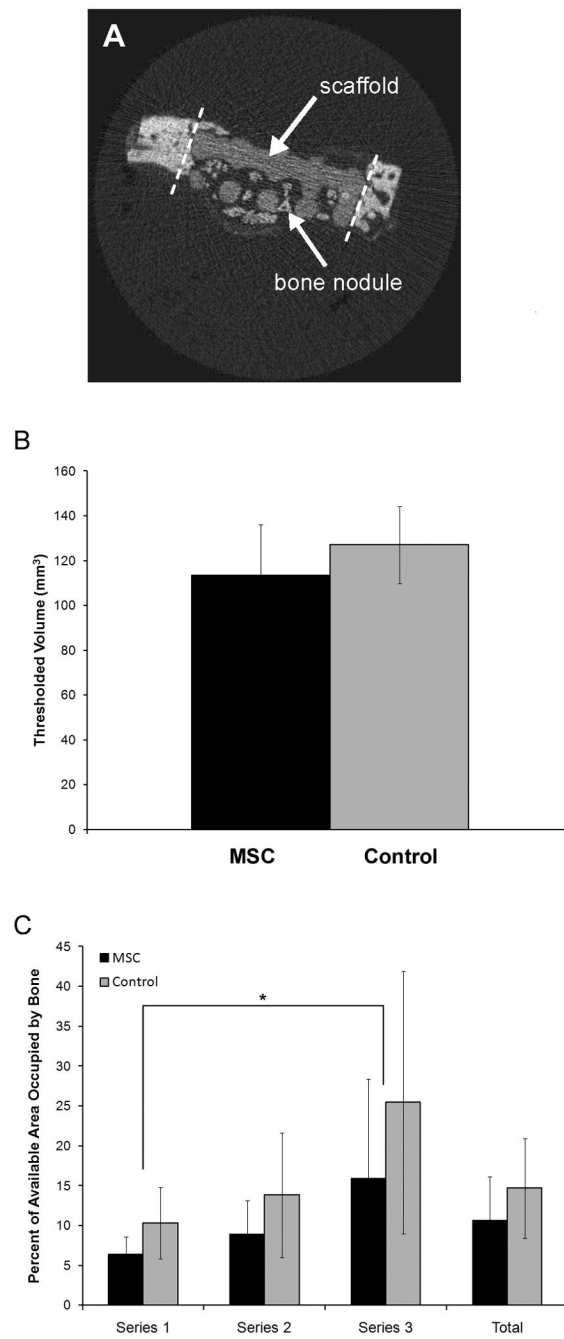


Figure 7.

**Table 1**

Results of Flow Cytometry Based Assay for Cytocompatibility.

	<b>% Viable</b>	<b>% Necrotic</b>	<b>% Early Apoptotic</b>	<b>% Dead by Apoptosis</b>
Control	96.23 ± 2.36	2.12 ± 0.48	0.39 ± 0.20	1.27 ± 1.75
PPF-DCPD	96.00 ± 0.19	3.59 ± 0.99	0.31 ± 0.08	0.09 ± 0.05